# Time domain simulation and sound synthesis for the snare drum

# Time domain simulation and sound synthesis for the snare drum

Stefan Bilbao[a)]
*Acoustics and Fluid Dynamics Group/Music, University of Edinburgh, Room 7306B, James Clerk Maxwell Building, King's Buildings, Mayfield Road, Edinburgh EH9 3JZ, United Kingdom*

(Received 25 November 2010; revised 2 March 2011; accepted 31 March 2011)

The snare drum is a complex system, relying on the interaction of multiple components: the drumheads, or membranes, a set of snares, the surrounding acoustic field and an internal cavity. Because these components are multidimensional, and due to a strong distributed non-linearity (the snare interaction), many techniques used frequently in physical modeling synthesis applications, such as digital waveguides and modal methods are difficult to apply. In this article, finite difference time domain techniques are applied to a full 3D system, and various features of interest, such as the coupling between membranes, and the interaction between the membranes and the snares, are examined in detail. Also discussed are various numerical features, such as spurious splitting of degenerate modes and bandwidth limitation, and estimates of computational complexity are provided. Sound examples are presented. © *2012 Acoustical Society of America*.
[DOI: 10.1121/1.3651240]

PACS number(s): 43.75.Hi, 43.75.Zz, 43.75.Wx, 43.40.Dx [NHF] Pages: 914–925

## I. INTRODUCTION

Percussion instruments have seen a fair amount of investigation at the experimental level, particularly regarding the determination of modal frequencies and shapes of complex structures.[1–3] To date, however, some of the more delicate features of such instruments, involving strong distributed nonlinearities (of geometric, and contact type), and multiple disparate interconnected components, have seen mainly experimental investigation,[4] without an underlying model of vibration (with some exceptions, in the case of gongs[5]). The scarcity of available models has made itself felt, not only in musical acoustics research, but also when it comes to sound synthesis based on physical models. The preeminent strategies used in physical modeling synthesis, such as digital waveguides and modal methods, are of relatively little use: waveguides, which are extremely efficient for linear problems in one dimension[6] are not well-suited to problems defined in multiple dimensions (though waveguide mesh structures have been used for drum synthesis[7,8]), and modal methods can become unwieldy, because of the presence of strong nonlinearities of distributed type, and because of the need for extensive offline calculation and storage (of modal shapes and frequencies). That being said, modal methods, in particular, have been used recently for efficient synthesis purposes, with good results.[9]

Time stepping strategies, such as finite difference schemes remain an approach capable of handling very general systems; due to great recent increases in computing power, it is no longer easy to rule out such techniques as too computationally intensive for synthesis for complex structures in a reasonable amount of time. This article is devoted to time domain simulation of coupled distributed systems, and in particular the snare drum, which serves as an excellent test case for the application of such methods to complex structures. While there is some work on such simulation techniques for similar systems, such as the kettledrum[10] in the context of pure musical acoustic research, here, the emphasis is on synthesis. In synthesis, there are many new issues which appear, including efficiency, the amount of offline calculation (as in the case of modal methods, as mentioned above), generality, and ease of programming; increasingly important, currently, is the ease with which a given algorithm may be parallelized, for implementation on a multicore processor, or graphics processing unit. All of these concerns have an influence on the choice of the particular type of time domain method to be employed, and will be explored in depth here. The synthesis viewpoint naturally leads one to simplify the various systems as much as possible, without degrading sound output; such simplifications (as well as examples of oversimplifications) will be presented in detail.

A model of a snare drum, written in terms of a coupled set of partial differential equations (PDEs) for the drum membranes, the acoustic field and the snares, is presented in Sec. II. Finite difference schemes, over uniform Cartesian grids, as well as their interconnection are introduced in Sec. III. Various issues, such as the choice of grid spacings, and interpolation, allowing the connection of disparate components, are discussed in detail. Simulation results, illustrating a number of features of interest in the case of the snare drum, such as membrane/membrane coupling, acoustic radiation, the all-important snare-membrane interaction, as well as numerical features such as spurious splitting of degerate modes, and bandwidth limitation, are given in Sec. IV. Various synthetic sound examples are also available on the author's website and as AIP Supplementary Material.[11]

## II. MODEL SYSTEM

In this section, the various components of the snare drum are described, in a continuous setting; finite difference operations are introduced in the following section.

[a)]Author to whom correspondence should be addressed. Electronic address: sbilbao@staffmail.ed.ac.uk

### A. Geometry

A snare drum cavity may be defined over a cylindrical region $\mathcal{V}_{int}$,defined by

$$\mathcal{V}_{int} = \{(x,y,z) \in \mathbb{R}^3 \big| x^2 + y^2 \leq R^2, |z| \leq L/2\}. \quad (1)$$

Here, $R$ is the drum radius, and $L$ is the height of the cavity, both in m. In simulation, it is also necessary to employ a computational region containing $\mathcal{V}_{int}$: in this case, a rectangular parallelepiped $\mathcal{V}$, defined as

$$\mathcal{V}_{ext} = \{(x,y,z) \in \mathbb{R}^3 || x|, |y| \leq L_{xy}/2, |z| \leq L_z/2\}, \quad (2)$$

for some lengths $L_{xy}$ and $L_z$, in m (and, for reasonable computation time, chosen not much larger than $R$ and $L$, respectively).

The boundary of the cavity $\partial\mathcal{V}_{int}$, may be decomposed as $\partial\mathcal{V}_{int} = \partial\mathcal{V}^{(b)} \cup \partial\mathcal{V}^{(s)} \cup \partial\mathcal{V}_{sh}$ where

$$\partial\mathcal{V}^{(b)} = \{(x,y,z) \in \mathbb{R}^3 \big| x^2 + y^2 \leq R^2, z = L/2\}, \quad (3a)$$

$$\partial\mathcal{V}^{(s)} = \{(x,y,z) \in \mathbb{R}^3 \big| x^2 + y^2 \leq R^2, z = -L/2\}, \quad (3b)$$

$$\partial\mathcal{V}_{sh} = \{(x,y,z) \in \mathbb{R}^3 \big| x^2 + y^2 = R^2, |z| \leq L/2\}. \quad (3c)$$

Here, $\partial\mathcal{V}^{(b)}$ and $\partial\mathcal{V}^{(s)}$ correspond to termination of the cylinder by the batter head and snare head, respectively, and $\partial\mathcal{V}_{sh}$ represents the termination of the sides of the drum by the shell. The boundary of the computational region $\mathcal{V}_{ext}$, consisting of six faces of a regular parallelepiped, is denoted $\partial\mathcal{V}_{ext}$. See Fig. 1.

### B. 3D acoustic wave propagation

The acoustic field, both inside the snare drum cavity, and outside (i.e., over the region $\mathcal{V}_{ext}$), is described by the 3D wave equation:

$$\Psi_{tt} = c^2 \Delta^{(3)} \Psi. \quad (4)$$

Here, $c$ is the wave speed in air, in m/s, $\Delta^{(3)}$ is the 3D Laplacian operator

$$\Delta^{(3)} = \frac{\partial^2}{\partial x^2} + \frac{\partial^2}{\partial y^2} + \frac{\partial^2}{\partial z^2}, \quad (5)$$

and $\Psi = \Psi(x, y, z, t)$ is the velocity potential of the acoustic field, both inside and outside the snare drum. Here, and elsewhere, the subscript $_{tt}$ indicates double partial differentiation with respect to time. The wave equation written in terms of the velocity potential is a more fundamental form than that written in terms of pressure,[12] and the resulting coupling to the membranes (see Sec. II F) is somewhat simplified. To this end, note that the acoustic pressure $p$ and the particle velocity v may be related to $\Psi$ through

$$p = \rho \Psi_t, \quad \mathrm{v} = -\nabla \Psi, \quad (6)$$

where $\rho$ is the density of air, $\nabla$ is the gradient operation, and where the subscript $t$ indicates partial differentiation

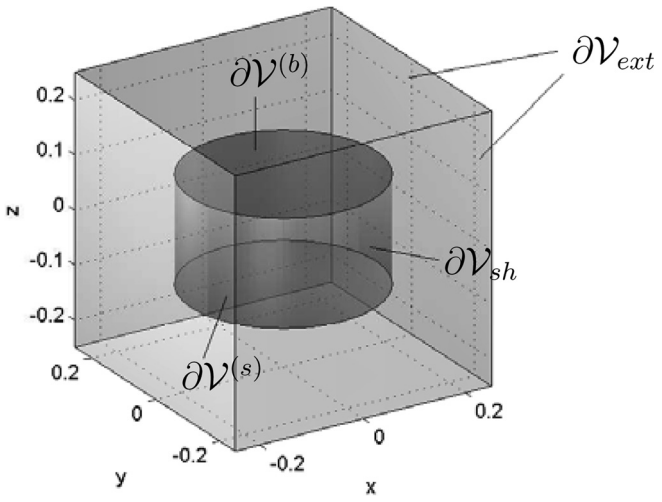


FIG. 1. Snare drum problem geometry, including computational region.

with respect to time. In this article, $c = 340$ m/s and $\rho = 1.2$ kg/m$^3$.

Boundary conditions for the snare drum shell, assumed rigid (not entirely realistic, as mentioned by Rossing *et al.*,[1] but a good first approximation), lead to Neumann type, or zero normal velocity conditions:

$$\mathbf{n}_{sh} \cdot \nabla \Psi = 0 \quad \text{over} \quad \partial\mathcal{V}_{sh}, \quad (7)$$

where $\mathbf{n}_{sh}$ is the normal to the shell boundary, both inside and outside the drum cavity. Boundary conditions for the membrane terminations will be discussed in Sec. II F.

An absorbing condition is required at the external boundary $\partial\mathcal{V}_{ext}$. There are many possible choices—among the most popular are so-called perfectly matched layers.[13,14] Such methods, though capable of absorbing impinging waves at all frequencies and angles of incidence, can require somewhat specialized computer implementation at the boundaries, and a fair increase in memory requirements, as the layer itself occupies three-dimensional space. In the interest of reducing programming complexity and memory requirements, for a problem which is already quite computationally demanding, various simpler absorbing boundary conditions, of Engquist-Majda type[15] have been examined here. Over the boundary $\partial\mathcal{V}_{ext}$ of the computational region, there is a series of such conditions, of increasing order of accuracy, expressed in terms of PDEs. The first two such conditions may be written as

$$\Psi_t + c\Psi_n = 0, \quad (8a)$$

$$\Psi_{tt} + c\Psi_{nt} - \frac{c^2}{2}(\Psi_{s_1 s_1} + \Psi_{s_2 s_2}) = 0, \quad (8b)$$

where a subscript $n$ indicates a spatial derivative outward normal to the boundary, and where subscripts $s_1$ and $s_2$ indicate tangential spatial derivatives. Higher order conditions are a possibility as well, but the above conditions are easily programmed and require little, if any extra memory requirement beyond that required to solve the problem over the interior.

### C. Membranes

The vibration of membranes will here be assumed to be fully transverse, a reasonable assumption for very thin structures. The dynamics of the two membranes (at the batter head and snare head), are described by

$$\rho^{(b)}H^{(b)}w_{tt}^{(b)} = T^{(b)}\Delta^{(2)}w^{(b)} + \cdots + f^{(b)} + f^{(exc)}, \tag{9a}$$

$$\rho^{(s)}H^{(s)}w_{tt}^{(s)} = T^{(s)}\Delta^{(2)}w^{(s)} + \cdots + f^{(s)} + f^{(snare)}, \tag{9b}$$

where here, $w^{(b,s)} = w^{(b,\ s)}(x, y, z)$ is the transverse displacement of each membrane, in m, $\rho^{(b,s)}$ is the density, in kg/m$^3$, $H^{(b,s)}$ is the thickness, in m, and $T^{(b,s)}$ the tension per unit length (assumed uniformly distributed over each membrane), in kg/s$^2$. $\Delta^{(2)}$ is the 2D Laplacian, defined as

$$\Delta^{(2)} = \frac{\partial^2}{\partial x^2} + \frac{\partial^2}{\partial y^2}. \tag{10}$$

The additional terms $f$ result from coupling. $f^{(b,s)}$ are the pressures due to the acoustic field on the batter head and the snare head, respectively, $f^{(exc)}$ results from the excitation, and $f^{(snare)}$ from the interaction with the snares. The precise forms of these terms will be given in Sec. II F.

The ellipses above indicate other higher-order terms which could be incorporated, with little resulting increase in programming complexity or computational cost in the resulting FDTD implementation. For example, for the batter head, in Eq. (9a) above, one could include the terms

$$-D^{(b)}\Delta^{(2)}\Delta^{(2)}w^{(b)} - \sigma_0^{(b)}w_t^{(b)} + \sigma_1^{(b)}\Delta^{(2)}w_t^{(b)} + \frac{6D^{(b)}}{\pi R^2 (H^{(b)})^2}\left(\int_{\partial\mathcal{V}^{(b)}} \left|\nabla w^{(b)}\right|^2 dA\right)\Delta^{(2)}w^{(b)}. \tag{11}$$

The first term, with $D^{(b)} = E(H^{(b)})^3/(12(1-(\nu^{(b)})^2))$, where $E^{(b)}$ and $\nu^{(b)}$ are Young's modulus and Poisson's ratio for the membrane, respectively, represents effects of stiffness; in the present case of a thin drum membrane, of generally quite low stiffness (for example, Young's modulus is approximately 4 GPa for Mylar, as opposed to 200 GPa for steel) the effect on the dynamics is quite small; modal frequencies and shapes deviate little from the non-stiff case, except at very high frequencies. The second and third terms, of coefficients $\sigma_0^{(b)}$ and $\sigma_1^{(b)}$, allow for frequency-dependent modeling of internal membrane losses; but given that radiation losses, modeled explicitly here through coupling to the acoustic field, are much larger, the resulting effect of these terms is rather small as well. The final term results from a simple averaged model of nonlinear membrane vibration, due to Berger,[16] and gives rise to the well-known pitch-glide phenomenon at high amplitudes,[17] similar to that which occurs in strings.[18] This term, incorporated in a recently proposed modal drum model,[9] is quite important perceptually in the case of certain drums, such as toms,[19] though it is anticipated to be much less so when a snare interaction is present, and the pitched quality of the resulting sound is suppressed.

The termination of the membranes at the shell boundary is assumed to be fixed, i.e.,

$$w^{(b,s)} = 0, \quad x^2 + y^2 = R^2. \tag{12}$$

If stiffness terms are included, second boundary conditions (clamped or pivoting) must be supplied for both membranes

In the simulation examples in Sec. IV, the densities of the batter head and snare heads are taken be 2690 and 2000 kg/m$^3$, respectively, and are of thicknesses 0.00013 m, and under tensions 3200 and 1500 N/m, respectively; such values were determined in the laboratory at Edinburgh, are in the range of values reported in the literature.[1]

### D. Snares

Attached to the snare head is a set of snares, which are tightly wound helical wires; such helical wires, in contrast to straight wires, exhibit string-like behavior (i.e., coherent wave propagation) at low frequencies.[20] A good first approximation is thus the 1D wave equation, describing motion of the snares in a direction normal to the membrane:

$$\rho^{(i)}A^{(i)}m_{tt}^{(i)} = T^{(i)}m^{(i)}_{\xi^{(i)}\xi^{(i)}} + f^{(i)} i = 1, \ldots, N^{(snare)}. \tag{13}$$

Here, $\rho^{(i)}$, $A^{(i)}$ and $T^{(i)}$ are the mass density, in kg/m$^3$, cross-sectional area, in m$^2$, and tension, in $N$ of a single snare (which may be assumed identical across all snares), and $m^{(i)}$ is the displacement of the $i$th snare (of which there are $N^{(snare)}$). $f^{(i)}$ is the force per unit length exerted on the $i$th snare due to interaction with the snare membrane. The forms of these terms will be given explicitly in Sec. II F.

The wave equations above are defined with respect to spatial coordinates $\xi^{(i)} \in [0, L^{(i)}]$, where $L^{(i)}$ is the length of the $i$th snare in m. In terms of the coordinates $x$ and $y$ on the membrane itself, assuming that the snares are parallel, and aligned with the $y$ direction, and are spaced apart by $\in$ m, the $i$th snare runs along coordinates

$$x^{(i)} = \frac{(2i - N^{(snare)} - 1)\in}{2}, \tag{14a}$$

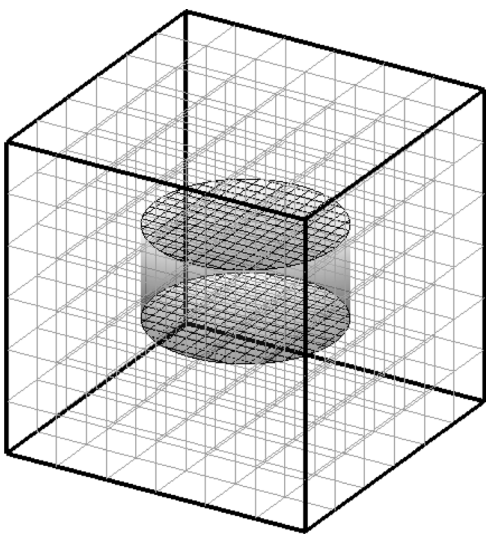

FIG. 2. Computational grid for the acoustic field, as well as for the membranes; the grid spacings are distinct.

$$y^{(i)} = y^{(i)}(\xi^{(i)}) = -L^{(i)}/2 + \xi^{(i)}. \tag{14b}$$

See Fig. 3. The ends of the snares are assumed attached to the membrane itself (a slight simplification from the actual situation, in which the snare ends are attached to a small rigid bar, which functions as a bridge). The termination conditions are thus

$$m^{(i)}(0) = w^{(s)}(x^{(i)}, \quad y^{(i)}(0)), \tag{15}$$

$$m^{(i)}(L^{(i)}) = w^{(s)}(x^{(i)}, \quad y^{(i)}(L^{(i)})). \tag{16}$$

As in the case of membranes, other terms (such as those involving internal damping) could well be included in Eq. (13) above.

### E. Excitation

For single strikes of strings or membranes, the typical model employed involves a nonlinear collision with a mass/spring system.[10,21] In this case, the term $f^{(exc)}$ in Eq. (9a) may be written as

$$f^{(exc)} = -F^{(m)}(t)\phi(x,y), \tag{17}$$

where $F^{(m)}$ is the force on the stick, and where $\phi(x, y)$ is a distribution, assumed fixed, representing the spatial extent of the contact region of the collision with the membrane. The dynamics of the stick itself, with an assumed initial velocity, may be written as[10]

$$F^{(m)} = M^{(m)}\frac{dw^{(m)}}{dt^2} \tag{18}$$

$$= K^{(m)}\left(\left[\int_{\partial\mathcal{V}^{(b)}} w^{(b)}\phi dA - w^{(m)}\right]^{+}\right)^{\alpha(m)}, \tag{19}$$

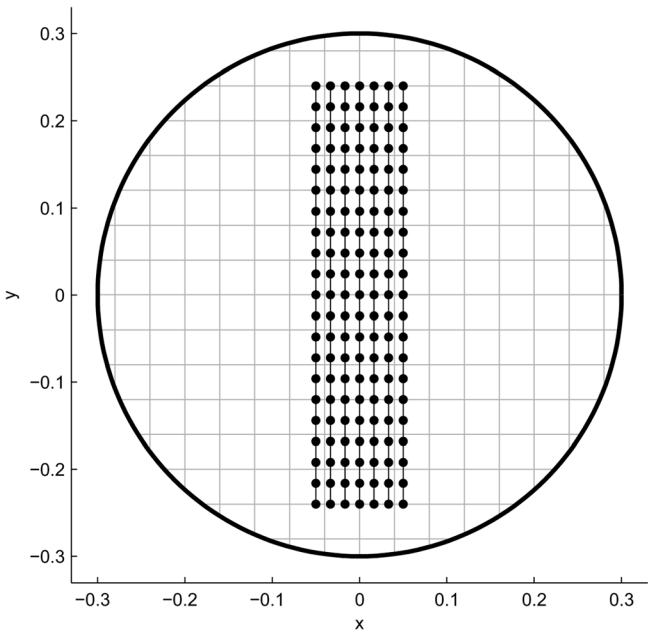


FIG. 3. Computational grid for the snare head, as well as 1D grids for a set of snares.

where $w^{(m)}(t)$ is the vertical displacement of the stick tip above the membrane, and where $M^{(m)}$, $K^{(m)}$ and $\alpha^{(m)}$ are the mass, stiffness constant, and nonlinear stiffness exponent associated with the stick. $[\cdot]^+$ indicates the "positive part of." Because the contact region is of dimensions which are very small compared to those of audible wavelengths in the membrane, it is sufficient in practice to use a 2D Dirac delta function (i.e., a distribution which integrates to unity over the surface of the membrane, and which selects the excitation point).

While such a model may easily be incorporated into a finite difference model, and adequately reproduces single strikes, it is not sufficient to replicate typical snare gestures, such as rolls, which require a more delicate model of the stick/membrane interaction. Such a model is as yet unapproached in the literature, and will require a continuous external applied force from the player (to maintain an autooscillation), and the ability of the stick to pivot.

For single strikes, a great simplification, in synthesis, is to simply specify $F^{(m)}$ as a short pulse, on the order of a millisecond in duration. One simple choice[22] is a function of the form

$$F^{(m)}(t) = \begin{cases} \frac{F_0}{2}(1 - \cos(2\pi t/T_0)) & 0 \le t \le T_0 \\ 0 & \text{else.} \end{cases} \tag{20}$$

The duration $T_0$ of the pulse, and amplitude $F_0$ may be roughly parameterized in terms of initial strike velocity: $F_0$ increases, and $T_0$ decreases as strike velocity increases.

Such a simplification is employed in the remainder of this article, because (a) it leads to great simplification in terms of programming, (b) reduces the risk of numerical instability, and (c) generates perceptually comparable, if not identical results in a synthesis setting, at least for single strikes. In the setting of musical acoustics, such a model is obviously not sufficient, but then, neither is the model presented above, in the case of continuous gestures, because of the deficiencies noted above.

### F. Distributed coupling

The system describing a snare drum is composed of various interacting components: the acoustic field, the two membranes, and the snares. In this section, the necessary coupling relations among the components are presented.

The coupling terms $f^{(b)}$ and $f^{(s)}$ in Eq. (9) may be written in terms of the velocity potential $\Psi$ as

$$f^{(b)} = \rho\left(\lim_{z\to\frac{L}{2}^-}\Psi_t - \lim_{z\to\frac{L}{2}^+}\Psi_t\right)\Big|_{\partial\mathcal{V}^{(b)}}, \tag{21a}$$

$$f^{(s)} = \rho\left(\lim_{z\to-\frac{L}{2}^-}\Psi_t - \lim_{z\to-\frac{L}{2}^-}\Psi_t\right)\Big|_{\partial\mathcal{V}^{(s)}}. \tag{21b}$$

The other required conditions relate membrane velocities to the gradient of the acoustic field, in the $z$ direction:

$$w_t^{(b)} = -\lim_{z\to\frac{L}{2}^-} \Psi_z\big|_{\partial\mathcal{V}^{(b)}} = -\lim_{z\to\frac{L}{2}^+} \Psi_z\big|_{\partial\mathcal{V}^{(b)}}, \tag{22a}$$

$$w_t^{(s)} = -\lim_{z\to-\frac{L}{2}^-} \Psi_z\big|_{\partial\mathcal{V}^{(s)}} = -\lim_{z\to-\frac{L}{2}^+} \Psi_z\big|_{\partial\mathcal{V}^{(s)}}, \tag{22b}$$

In summary: the pressure exerted on a membrane is the difference of the pressures exerted on either side, and the particle velocity of the acoustic field normal to a membrane must be equal to the membrane velocity, on either side of the membrane.

Coupling between the snare membrane and the snares involves distributed partial collisions. A useful model is similar to that of a hammer interaction (see Sec. II E) along the length of the snare. For the i*th* snare,

$$f^{(i)} = -K^{(i)}\left([m^{(i)} - w^{(s)}(x^{(i)}, y^{(i)})]^+\right)^{\alpha^{(i)}}, \tag{23}$$

where $K^{(i)}$ and $\alpha^{(i)}$ are a compression coefficient and nonlinear exponent for the *i*th snare. The coordinates $x^{(i)}$ and $y^{(i)}$ along the membrane are as given in Eq. (14). The total force exerted on the snare membrane, $f^{(snare)}$ is thus

$$f^{(snare)} = -\sum_{i=1}^{N^{(snare)}} f^{(i)}\delta(x(\xi^{(i)}), \quad y(\xi^{(i)})), \tag{24}$$

where $\delta(x^{(i)}, y^{(i)})$ is the Cartesian product of a 1D Dirac delta function with the linear region of the membrane over which the *i*th snare is in partial contact.

This is a somewhat ad hoc model of snare collision; ideally, one would prefer a model for which collision is rigid; this formalism, when the stiffness coefficients $K^{(i)}$ are chosen large, approaches the ideal, while allowing numerical difficulties associated with rigid collision to be sidestepped.

### G. Simplified piston model

In the interest of reducing computational cost, and also of simplifying analysis in the problem of coupled membranes, piston models of the air cavity have been proposed.[1,9] The air cavity is modeled as a uniform slug, with a given mass and stiffness. A coupled membrane PDE model may be adapted from a standard one membrane cavity model, and is of the form given in Eq. (9), where the coupling terms $f^{(b)}$ and $f^{(s)}$ are written as

$$f^{(b)} = -f^{(s)} = \frac{\rho c^2}{|\mathcal{V}_{int}|}\left(\int_{\partial\mathcal{V}^{(s)}} w^{(s)}dA - \int_{\partial\mathcal{V}^{(b)}} w^{(b)}dA\right). \tag{25}$$

This model is thus written purely in terms of the membrane displacements $w^{(b)}$ and $w^{(s)}$, but now, radiation effects have been neglected [and must be reintroduced, through additional terms in Eq. (9)].

One expects that such a model will indeed lead to interaction of modes between the upper and lower membranes, and also that a perceptually important attribute of the resulting sound will be lost, namely the cavity modes, which, in the full 3D case, become increasingly dense towards the high end of the audio spectrum. See Sec. IV E for further discussion of this simplification, and comparison with the 3D case, with regard to the effect on snare motion.

## III. FINITE DIFFERENCE SCHEMES

In this section, finite difference schemes for the various coupled subsystems are introduced. The emphasis here is on sound synthesis, and operation at a reasonable audio sample rate $f_s$ (such as 44.1 kHz). Because the problem is defined over a cylindrical geometry, it is tempting to conclude that schemes in radial coordinates are a good match, at least for the membrane components and the acoustic field. Unfortunately, however, explicit schemes in radial coordinates exhibit extremely poor frequency domain behavior, including severe numerical dispersion, and, what is worse, bandlimiting of responses over a small range of frequencies (in the present case of the snare drum, down to 3 kHz, even if the scheme operates at 44.1 kHz). This issue is discussed in detail in a recent book.[23] The bandlimiting effect is especially important in the case of nonlinear snare/membrane coupling, which generally introduces high-frequency energy, which the membrane must be capable of supporting (and thus, radiating). See IV A for some exploration of this.

Though one can use such schemes (perhaps at a higher sampling rate, or involving computationally costly implicit updates), for audio synthesis purposes, it is more useful to employ schemes over multiple Cartesian grids, even if additional issues relating to the termination of the grid over a cylindrical geometry intervene (such as irregular boundary termination). Such regular schemes, especially over the 3D acoustic field, are also a very good match to parallel computer architectures—updates are performed identically at each point in the domain interior. This is in contrast with the case of pure musical acoustics applications, where other choices, such as finite element/finite volume methods, over irregular grids could give better results, especially with regard to irregular boundary conditions.[10]

The schemes for all components presented in this section will operate at a uniform sample rate of $f_s$, and for which $t_s = 1/f_s$ is the time step; grid spacings, however, will in general be different for the various components. Second time derivatives of quantities $g_{tt}(\cdot, t)$, which appear in the defining equations of all the various components will be approximated here uniformly by

$$\frac{1}{t_s^2}(g_\cdot^{n+1} - 2g_\cdot^n + g_\cdot^{n-1}) \approxeq g_{tt}, \tag{26}$$

where $g_\cdot^n$ is an approximating grid function for $g(\cdot,t)$ at time $nt_s$, for integer $n$.

### A. Schemes for components

A simple finite difference time domain scheme for the 3D wave Eq. (4) is the following:

$$\Psi_{l,m,p}^{n+1} = (2 + c^2 t_s^2 \delta^{(3)})\Psi_{l,m,p}^n - \Psi_{l,m,p}^{n-1}. \tag{27}$$

Here, $\psi_{l,m,p}^n$ represents an approximation to $\Psi(x, y, z, t)$, at times $t = nt_s$, where $t_s$ is the time step, and at grid points indexed by $l$, $m$ and $p$, separated from one another by a grid

spacing $h$. See Fig. 2. A seven point approximation to the 3D Laplacian, $\delta^{(3)}$, is given by

$$\delta^{(3)}\Psi^n_{l,m,p} = \frac{1}{h^2}\Big(\Psi^n_{l+1,m,p} + \Psi^n_{l-1,m,p} + \Psi^n_{l,m+1,p} + \Psi^n_{l,m-1,p} + \Psi^n_{l,m,p+1} + \Psi^n_{l,m,p-1} - 6\Psi^n_{l,m,p}\Big). \tag{28}$$

A necessary stability condition for scheme, Eq. (27), follows, from von Neumann analysis,[24] as

$$h \geq h_{min} = \sqrt{3}ct_s. \tag{29}$$

For the least numerical dispersion, it is generally wise to choose $h$ (given the time step $t_s$) as close to $h_{min}$ as possible. Geometric constraints intervene, however—for a simple implementation of the membrane coupling conditions, Eq. (21) and (22), it is useful to choose the grid spacing such that the membranes (at heights $z = \pm L/2$) lie exactly halfway between adjacent grid points, and thus an additional constraint is that $L/h$ be an integer. This leads to a minor deviation of $h$ from $h_{min}$.

Schemes for the membranes, as defined in Eq. (9), are similar; assuming, for simplicity, that the various additional terms given in, Eq. (11), are neglected, simple schemes are:

$$(w^{(b)})^{n+1}_{l,m} = (2 + (c^{(b)})^2 t_s^2 \delta^{(2,b)})(w^{(b)})^n_{l,m} - (w^{(b)})^{n-1}_{l,m} + \frac{t_s^2}{\rho^{(b)}H^{(b)}}\Big((f^{(b)})^n + (f^{(exc)})^n\Big), \tag{30a}$$

$$(w^{(s)})^{n+1}_{l,m} = (2 + (c^{(s)})^2 t_s^2 \delta^{(2,s)})(w^{(s)})^n_{l,m} - (w^{(s)})^{n-1}_{l,m} + \frac{t_s^2}{\rho^{(s)}H^{(s)}}\Big((f^{(s)})^n + (f^{(snare)})^n\Big). \tag{30b}$$

Here, $\left(w^{(b,s)}\right)^n_{l,m}$ is an approximation to $(w^{(b,s)})(x,y,t)$ at coordinates $x = h^{(b,s)}l$, $y = h^{(b,s)}m$ and at time $t = nt_s$, and the wave speeds $c^{(b,s)}$ are defined by $c^{(b,s)} = \sqrt{T^{(b,s)}/\rho^{(b,s)}H^{(b,s)}}$. $\delta^{(2,b)}$ and $\delta^{(2,s)}$ are five-point approximations to the 2D Laplacian, defined by

$$\delta^{(2,q)}(w^{(q)})^n_{l,m} = \frac{1}{(h^{(q)})^2}\Big((w^{(q)})^n_{l+1,m} + (w^{(q)})^n_{l-1,m} + (w^{(q)})^n_{l,m+1} + (w^{(q)})^n_{l,m-1} - 4(w^{(q)})^n_{l,m}\Big), \tag{31}$$

where $q$ is either $b$ or $s$. Notice that the grid spacings $h^{(b)}$ and $h^{(s)}$ are in general distinct for the two membranes.

Necessary stability conditions for the schemes, Eq. (30), are

$$h^{(b,s)} \geq h^{(b,s)}_{min} = \sqrt{2}c^{(b,s)}t_s, \tag{32}$$

and should be satisfied as close to equality as possible for minimal numerical dispersion, and maximal bandwidth. If stiffness terms [see Eq. (11)] are included, the bound above must be altered—and in general, $h^{(b,s)}_{min}$ increases, leading to a decrease in memory requirements. See Fig. 3.

Similarly, for the systems, Eq. (13), for the snares, one may write the schemes

$$(m^{(i)})^{n+1}_l = 2m(m^{(i)})^n_l - (m^{(i)})^{n-1}_l + (c^{(i)})^2 t_s^2 \delta^{(1,i)}(m^{(i)})^n_l + \frac{t_s^2}{\rho^{(i)}A^{(i)}}(f^{(i)})^n \quad i = 1, \ldots, N^{(snare)}, \tag{33}$$

where $\left(m^{(i)}\right)^n_l$ is an approximation to $m^{(i)}(\xi^{(i)}, t)$, at $= \xi^{(i)} = lh^{(i)}$, and $t = nt_s$, and where $c^{(i)} = \sqrt{T^{(i)}/\rho^{(i)}A^{(i)}}$. The second difference operator $\delta^{(i,1)}$ is defined as

$$\delta^{(i,1)}(m^{(i)})^n_l = \frac{1}{(h^{(i)})^2}\Big((m^{(i)})^n_{l+1} - 2(m^{(i)})^n_l + (m^{(i)})^n_{l-1}\Big). \tag{34}$$

See Fig. 3

Necessary stability conditions for the schemes, Eq. (33), are that

$$h^{(i)} \geq h^{(i)}_{min} = c^{(i)}t_s. \tag{35}$$

### B. Boundary termination

Boundary termination of scheme, Eq. (27), for the 3D wave equation at the shell boundary $\partial\mathcal{V}_{sh}$ may be carried out through a simple "staircase" approximation. See Fig. 4.

At points adjacent to $\partial\mathcal{V}_{sh}$, the simplest approximation to the Neumann condition, Eq. (7), is to reflect values required on the other side of the boundary back to the central update point without sign inversion. Referring to Fig. 4, the update at point labeled A requires two such virtual values (i.e., values outside the interior of the drum cavity in this case), and that at point B requires one.

At point A, the Laplacian may be approximated as

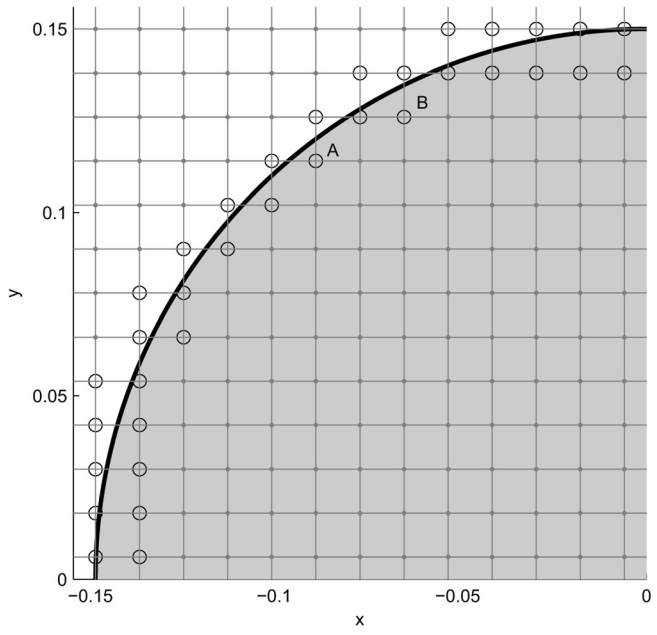


FIG. 4. Computational grid for the acoustic field, viewed from above, with the shell boundary $\partial\mathcal{V}_{sh}$ indicated as a dark circle. Points at which specialized updating must be performed are indicated by open circles.

$$\delta^{(3)}\Psi^n_{l,m,p} = \frac{1}{h^2}\Big(\Psi^n_{l+1,m,p} + \Psi^n_{l,m-1,p} + \Psi^n_{l,m,p+1} + \Psi^n_{l,m,p-1} - 4\Psi^n_{l,m,p}\Big), \quad (36)$$

and at point B,

$$\delta^{(3)}\Psi^n_{l,m,p} = \frac{1}{h^2}\Big(\Psi^n_{l+1,m,p} + \Psi^n_{l,m-1,p} + \Psi^n_{l-1,m,p} + \Psi^n_{l,m,p+1} + \Psi^n_{l,m,p-1} - 5\Psi^n_{l,m,p}\Big). \quad (37)$$

Numerical boundary conditions at $\partial\mathcal{V}_{ext}$, at which an absorbing boundary condition is applied, may also be easily arrived at. For condition, Eq. (8a), for example, at a point on the upper face of $\partial\mathcal{V}_{ext}$, one possible update, obtained through centered discretization and insertion in Eq. (27), is

$$\Psi^{n+1}_{l,m,p} = \frac{\lambda^2}{1+\lambda}\Big((2/\lambda^2 - 6)\Psi^n_{l,m,p} + \Psi^n_{l+1,m,p} + \Psi^n_{l-1,m,p} + \Psi^n_{l,m+1,p} + \Psi^n_{l,m-1,p} + 2\Psi^n_{l,m,p-1} - (1/\lambda^2)\Psi^{n-1}_{l,m,p}\Big), \quad (38)$$

where $\lambda = ct_s/h$. This condition can be generalized, through symmetry, at all other faces, and requires a specialized form at the domain corners. A similar, slightly more complex update may be derived starting from condition, Eq. (8b), but is omitted here. Neither method requires an absorbing numerical layer.

Numerical fixed boundary conditions for the membranes, as given in Eq. (12) may be implemented, in the simplest instance, by setting grid values at points outside $\partial\mathcal{V}^{(b,s)}$ to be zero, or, for greater accuracy, through interpolation. As seen in Sec. IV A, this has a negligible effect on calculated modal frequencies, except at the upper end of the audio frequency range.

### C. Coupling and interpolation

The various schemes for the acoustic field, membranes, and snares all operate over grids of distinct spacings, and thus the coupling relations described in Sec. II F must be approached via some form of interpolation.

Consider first the coupling between the upper membrane (the batter head) and the acoustic field, defined over grids of spacings $h^{(b)}$ and $h$, respectively. It is necessary to define two interpolants $\mathcal{I}^{h\to h(b)}$ and $\mathcal{I}^{h(b)\to h}$, operating from a 2D subset of the acoustic field values to the membrane, and vice versa. Interpolation between distributed coupled systems, is described in a recent book.[25] A simple choice in either case is bilinear inerpolation. The coupling Eq. (21a) may be discretized as

$$(f^{(b)})^n = \rho\mathcal{I}^{h\to h^{(b)}}\frac{\Psi^{n+1}_{\cdot,p^{(b)}} - \Psi^{n-1}_{\cdot,p^{(b)}}}{2t_s} - \rho\mathcal{I}^{h\to h^{(b)}}\frac{\Psi^{n+1}_{\cdot,p^{(b)}+1} - \Psi^{n-1}_{\cdot,p^{(b)}+1}}{2t_s}, \quad (39)$$

where $\Psi^n_{\cdot,p^{(b)}}$ and $\Psi^n_{\cdot,p^{(b)}+1}$ indicate the grid points for the acoustic field directly adjacent to the membrane, below and above, respectively.

Updating $\Psi^n_{l,m,p}$, according to scheme, Eq. (27), at $p = p^{(b)}$, and $p = p^{(b)} + 1$, requires access, apparently, to values of the grid function on the other side of the membrane; call these virtual grid values $\Psi^{*,n}_{\cdot,p^{(b)}}$ and $\Psi^{*,n}_{\cdot,p^{(b)}+1}$. Coupling conditions, Eq. (22a), may be discretized as

$$\mathcal{I}^{h^{(b)}\to h}\frac{(w^{(b)})^{n+1} - (w^{(b)})^{n-1}}{2t_s} = -\frac{\Big(\Psi^{*,n}_{\cdot,p^{(b)}+1} - \Psi^n_{\cdot,p^{(b)}}\Big)}{h} = -\frac{\Big(\Psi^n_{\cdot,p^{(b)}+1} - \Psi^{*,n}_{\cdot,p^{(b)}}\Big)}{h}. \quad (40)$$

In implementation, conditions, Eq. (40), may be used to solve for the virtual grid values $\Psi^{*,n}_{\cdot,p^{(b)}}$ and $\Psi^{*,n}_{\cdot,p^{(b)}+1}$, which may then be used directly in schemes, Eqs. (27) and (30), leading to a fully explicit update.

The coupling conditions for the snares also require interpolation. Supposing $\mathcal{I}^{h^{(s)}\to h^{(i)}}$ is an interpolant from values on the grid for the snare head to the corresponding positions along the ith snare (possibly bilinear), then condition, Eq. (23), may be discretized as

$$(f^{(i)})^n = -K^{(i)}\left(\left[(m^{(i)})^n - \mathcal{I}^{h^{(s)}\to h^{(i)}}(w^{(s)})^n\right]^+\right)^{\alpha^{(i)}}. \quad (41)$$

Defining an extrapolant $\mathcal{I}^{h^{(i)}\to h^{(s)}}$ from the ith snare to grid locations on the snare head, again, perhaps, bilinearly, so that values are distributed to adjacent grid locations on the membrane grid, then condition, Eq. (24), may be discretized as

$$(f^{(snare)})^n = -\sum_{i=1}^{N^{(snare)}}\mathcal{I}^{h^{(i)}\to h^{(s)}}(f^{(i)})^n. \quad (42)$$

The snare coupling conditions are nonlinear; as such, one should expect some danger of instability, especially if the stiffness coefficients $K^{(i)}$ for the snares are high; a good remedy involves semi-implicit schemes applied to Eq. (41).

### D. Computational cost

Computational cost is dominated by the solution of the scheme for the 3D wave, Eq. (27), and those for the two membranes, Eq. (30). Memory requirements $N^{(3D)}$ and $N^{(b,s)}$ follow directly from the stability conditions, Eqs. (29) and (32). For a given sample rate $f_s = 1/t_s$, and for two step schemes, these may be written as

$$N^{(3D)} = \frac{2|\mathcal{V}_{ext}|f_s^3}{3^{3/2}c^3}, \quad N^{(b,s)} = \frac{\pi R^2 f_s^2}{(c^{(b,s)})^2}. \quad (43)$$

The memory requirement for the membranes is a worst case; if stiffness effects are included (see Sec. III A), then the grid spacing will increase, and memory requirements will thus decrease.

The operation counts per second $O^{(3D)}$ and $O^{(b,s)}$, for two-step finite difference schemes will be, again assuming that stiffness is neglected in membranes,

$$O^{(3D)} = 4N^{(3D)}f_s, \quad O^{(b,s)} = 3N^{(b,s)}f_s. \tag{44}$$

In the limit of high sample rates, then, the total operation count will be dominated by $O^{(3D)}$, which scales with the fourth power of the sample rate. For typical snare membrane parameters, and at an audio sample rate of $f_8 = 44\,100$ kHz, and using a small computational region, of $|\mathcal{V}_{ext}| = 0.5^3$ m$^3$, one has

$$O^{(3D)} = 1.85 \times 10^{10}, \quad O^{(b,s)} = 2.89 \times 10^9, \tag{45}$$

These values are large, but given that typical computer processors now operate at the GHz rate, one should expect that an efficiently programmed implementation should operate near real time, especially if the implementation is multithreaded. Indeed, the use of Cartesian schemes is far more amenable to parallelization than, e.g., schemes in radial coordinates, because updates are uniform over the problem space, both for the 3D region and the membranes. In addition, the use of a rectangular parallelepiped as the main computational region makes for a very good fit to highly parallel architectures such as GPUs (Ref. 25). On the other hand, special indexing strategies will be required in order to represent the cylindrical region over such a grid. It is also interesting to note that because wave speeds in drum membranes are generally much lower than in air, the computational cost of the membrane solution is not negligible compared to that of the 3D problem, for small computational regions, at typical audio sample rates, as mentioned above.

## IV. SIMULATION RESULTS

In this section, the aim is to demonstrate various features of snare drum vibration, and in particular those which it may not be possible to simulate using simplified models, as well as inevitable numerical artifacts of a finite difference treatment. Among these are a comparison between numerical results obtained using radial and Cartesian grids, the complex behavior of modal frequencies of a coupled membrane system, acoustic radiation, the snare interaction, including a comparison between results obtained using the full 3D model, and those obtained using a simplified piston model.

All simulation results presented in this section are carried out for a drum with radius $R = 0.15$ m, and of a height of $L = 0.3$ m, unless otherwise indicated. A set of twelve snares is employed, of length $L^{(i)} = 0.25$ m, and with wave speed $c^{(i)} = 30$ m/s, attached to the snare head over a band of width 0.05 m. Such parameters correspond roughly to those of a drum in the laboratory at Edinburgh. Parameters for the acoustic field and for the membranes are as given in Secs. II B and II C, respectively.

### A. Radial and cartesian schemes

As a preliminary justification for the use of rectangular grids, consider the case of a membrane, in isolation, without stiffness. In this case, the displacement of the membrane satisfies the 2D wave equation, over a circle of radius $R$, with fixed boundary conditions. In Table I, a comparison between exact modal frequencies, and those calculated by a scheme over a Cartesian grid, and another scheme over a grid in radial coordinates is given; both schemes are run at a sample rate of 44.1 kHz, with grid spacings chosen as close to the stability condition, Eq. (32), as possible for the Cartesian scheme. Though both schemes perform well at low frequencies, the radial scheme exhibits severe dispersion in the range above approximately 1 kHz. Furthermore, as illustrated in Fig. 5, the output of the radial scheme is bandlimited to approximately 3 kHz. Though such schemes are used in investigations in musical acoustics, it is clear that the radial scheme will be unable to give a good approximation to the dynamics of the snare system at high frequencies, at reasonable audio sample rates.

TABLE I. Exact modal frequencies, in Hertz, for a circular membrane, with radius $R = 0.15$ m and wave speed $c = 95.63$ m/s, with fixed boundary conditions, and frequencies calculated by schemes in Cartesian coordinates, and radial coordinates. Numerical modal frequencies are obtained through frequency domain (i.e., eigenvalue) analysis of the discretized spatial operators in conjunction with a two step scheme in either case.

| Mode number | Exact | Cartesian | Radial |
|---|---|---|---|
| 1 | 244.2 | 244.3 | 243.6 |
| 2 | 389.0 | 389.2 | 387.6 |
| 3 | 521.3 | 521.8 | 518.4 |
| 4 | 560.4 | 560.8 | 554.4 |
| 5 | 647.7 | 648.2 | 641.6 |
| 40 | 1984.8 | 1988.5 | 1641.8 |

On the other hand, schemes in regular Cartesian coordinates can introduce artifacts of their own. In the present case of the circular membrane, one such artifact is splitting of degenerate modes, as illustrated in Fig. 6; this is an entirely numerical effect, and is due to the lack of radial symmetry of the grid. Such splitting, leading to closely spaced pairs of modal frequencies, could potentially lead to audible beating

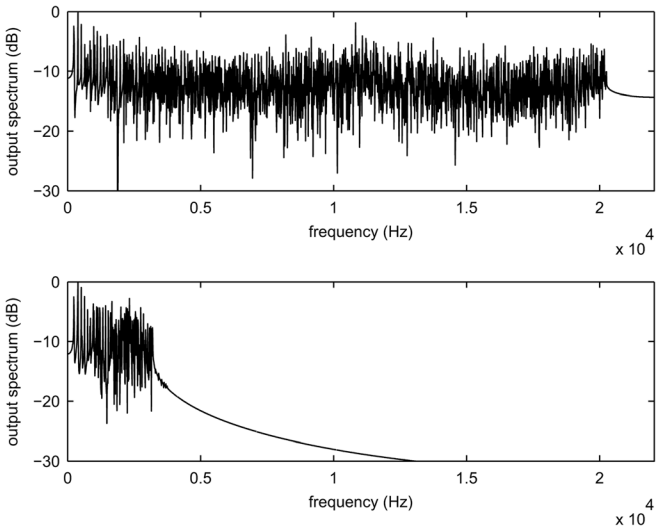


FIG. 5. Output responses, for a scheme operating over a Cartesian grid (top) and over a radial grid (bottom).

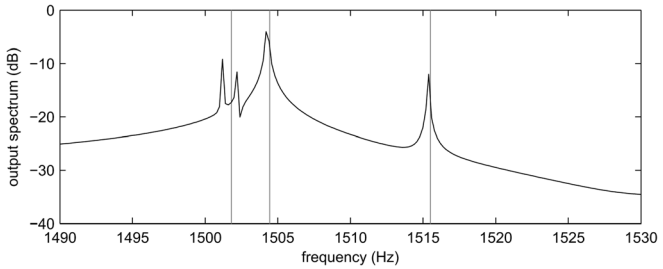


FIG. 6. A region of the output spectrum, for a circular membrane, of radius $R = 0.15$ m, and with wave speed $c = 95.63$ m/s, illustrating a numerically split degenerate mode pair at approximately 1502 Hz. Exact modal frequencies are shown as grey lines.

effects—but in the case of the snare drum, it is likely that such effects will be masked entirely by the noise-like character of the resulting sound

### B. Coupled membrane interaction

The coupled acoustic field/membrane/membrane scheme allows the explicit investigation of coupling between modes in the upper and lower membranes. Indeed, for analysis purposes, a time stepping algorithm is not necessary; provided one has consolidated all of the spatial discretization terms in matrices, a standard eigenvalue solver is a possibility, though such techniques will obviously not be of use in synthesis when distributed nonlinearities such as the snare mechanism are present. A full simulation, however, is revealing, even in the linear case when the snares are disengaged—see Fig. 7, showing the response of the system to an impulsive excitation applied at a point off center on the batter head. Visible is the slight delay in the excitation of the snare head, as well as the concentration of much of the vibration of the snare head in axisymmetric modes.

As a numerical experiment, it is interesting to look at the complex trajectories of modal frequencies for the coupled system, under increases in mass density of the membranes, as shown in Fig. 8. In the limit of high densities, the frequencies of the coupled system separate into those of two uncoupled membranes, as expected.

### C. Acoustic radiation

In Fig. 9, the time evolution of a vertical cross section of the acoustic field is shown, when the batter head is again subjected to an impulsive excitation. Spurious reflection from the computational boundary is not evident.

### D. Snare interaction

The interaction of the snares with the snare head is enormously complex; so dependent is it on the interaction between the membranes, that it is difficult to envisage how to simplify the model without losing perceptually important features (though this has indeed been attempted, by Avanzini *et al.*[9] using lumped approximations to the snares themselves).

Figure 10 illustrates this motion. Because it is mainly the axisymmetric modes of the snare head which are excited, through a strike on the batter head and the subsequent propagation of acoustic waves through the drum cavity, initially the motion of the snares is relatively coherent; once recontact is made between the snares and the snare head, the motion is quickly randomized, leading directly to the noise-like timbre of the snare drum. The degree of randomization is influenced strongly by asymmetric mode coupling between the membranes, as discussed in the following section. Also shown, in Fig. 11, is the launch of a single snare from the snare head, in profile, as well as subsequent recontact; notice that the motion of the snare is slightly asymmetric about its center, even after a single bounce off the snare head.

### E. Piston model

Simplified models of the cavity, such as, e.g., a single mode model,[9] equivalent to that given here in Sec. II G, or a two-mass model such as that presented by Rossing *et al.*,[1] or indeed any model which includes only axisymmetric cavity modes, will not allow the transmission of energy between asymmetric modes for the two membranes. The motion of the snares will be far less randomized, even over very short time scales (indeed, the motion of each snare, in this case, will necessarily be symmetric about its midpoint!).

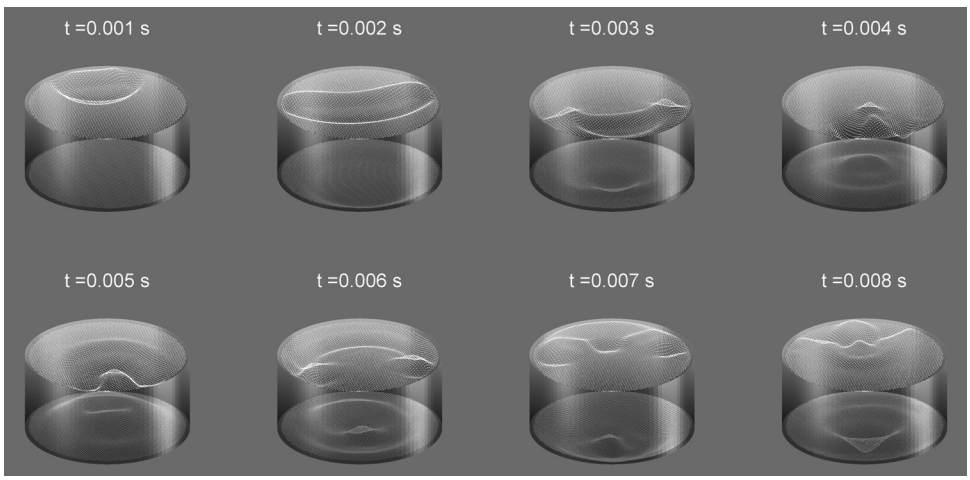


FIG. 7. Snapshots of the response of a coupled membrane system (with snares dis engaged) to an short impulsive excitation, viewed from above, at times as indicated.

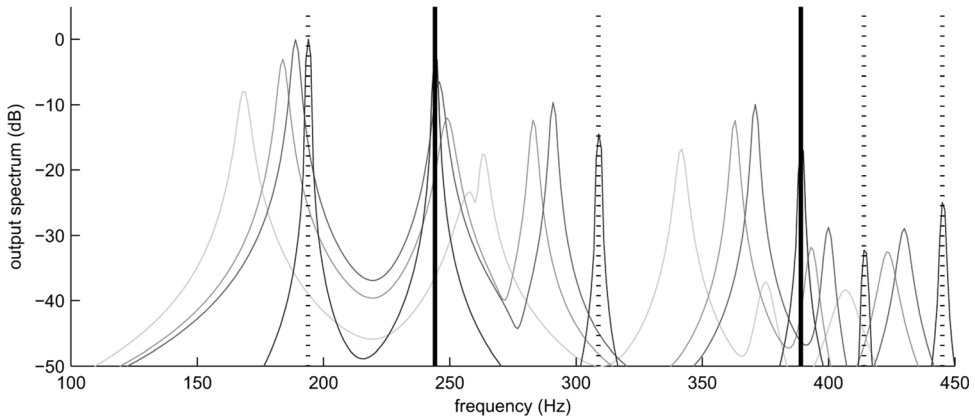


FIG. 8. Output spectrum of displacement drawn from a point on the snare membrane, due to an impulsive strike on the batter head, for four different membrane mass densities. In increasingly dark shades of grey, the spectrum of the response for densities of 1, 2, 3 and 1000 times the nominal densities of 2690 kg/m$^3$ and 2000 kg/m$^3$. Exact modal frequencies for the snare head and batter head, in isolation, are shown as dotted and solid vertical lines, respectively.

Compare, for example, the motion of a single snare in the case of a piston model as illustrated in Fig. 12, to that of the full 3D model, as in Fig. 11; the displacements for the two models do not match one another well. Although such simplified, or "lumped" cavity models may be useful in the context of drums without snares, in synthesis, they may be of doubtful utility. Sound examples produced using a simple one-mass, or piston model of the cavity are noticeably less realistic than those produced using a full 3D model, as the reader may verify—see Sec. IV F; this is due partly to the lack of randomness in the snare contact, as well as the lack of cavity modes, both of which play a crucial role in defining the timbre of the snare drum.

### F. Sound examples

Various sound examples, illustrating typical snare gestures, are available on the author's website, and as AIP Supplementary Material. Sound output is drawn, in stereo, from two locations 2 cm from the snare head, at symmetric locations about the drum center. Also included, for the sake of comparison, are sound examples produced using a simplified one-mass model of the cavity.

## V. CONCLUDING REMARKS

In this article, simulation of a complex multi-component instrument has been attempted, with the goal of producing synthetic sound—the main point here is that though computationally intensive, time-stepping methods are an excellent match to such problems, and do not require any undue model simplification (as, for example, in the case of the simplified piston model, which leads to a decrease in computational complexity, but for which for which sound synthesis results are very poor indeed).

Although the main emphasis here is on synthesis, this work could see use in musical acoustics investigations; the analysis of the motion of snares in a 3D model, as compared with the more commonly seen piston model is revealing in the discrepancy (and perceptual differences in sound synthesis results are even more striking). It is also possible that this tool may be used in conjunction with experimental

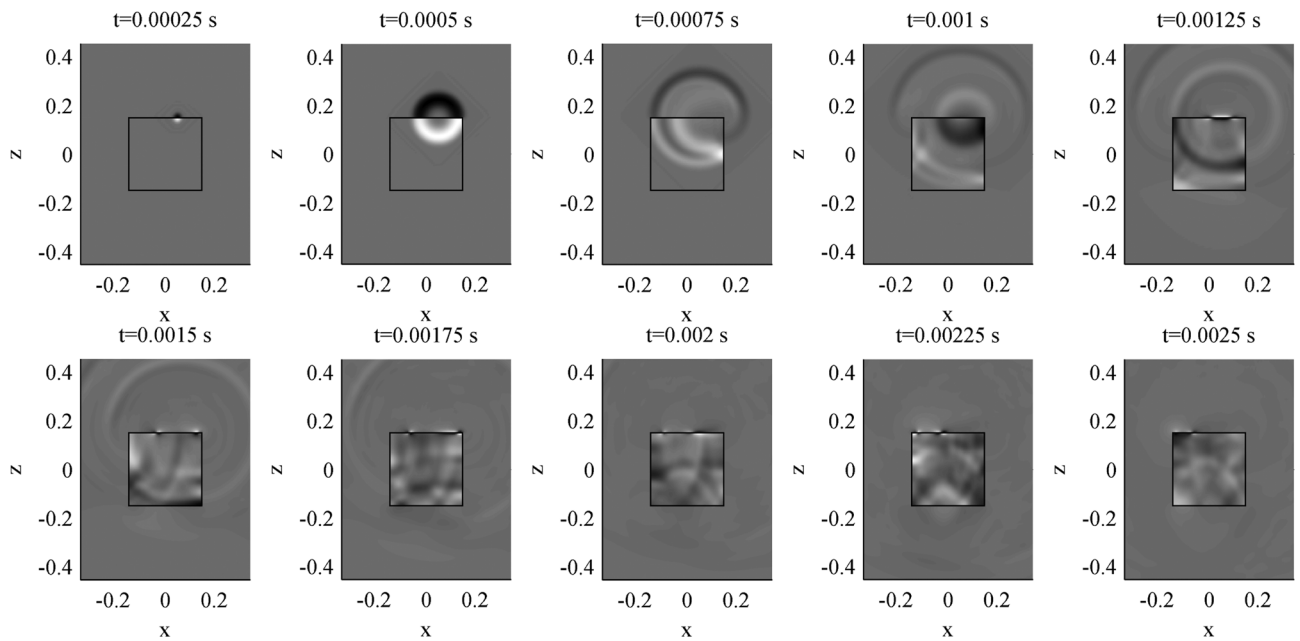


FIG. 9. Snapshots of a vertical cross-section of the acoustic field generated by a short impulsive excitation applied to the batter head, at times as indicated. Snares are disengaged. The boundary $\partial\mathcal{V}_{int}$ is shown as a dark rectangle.

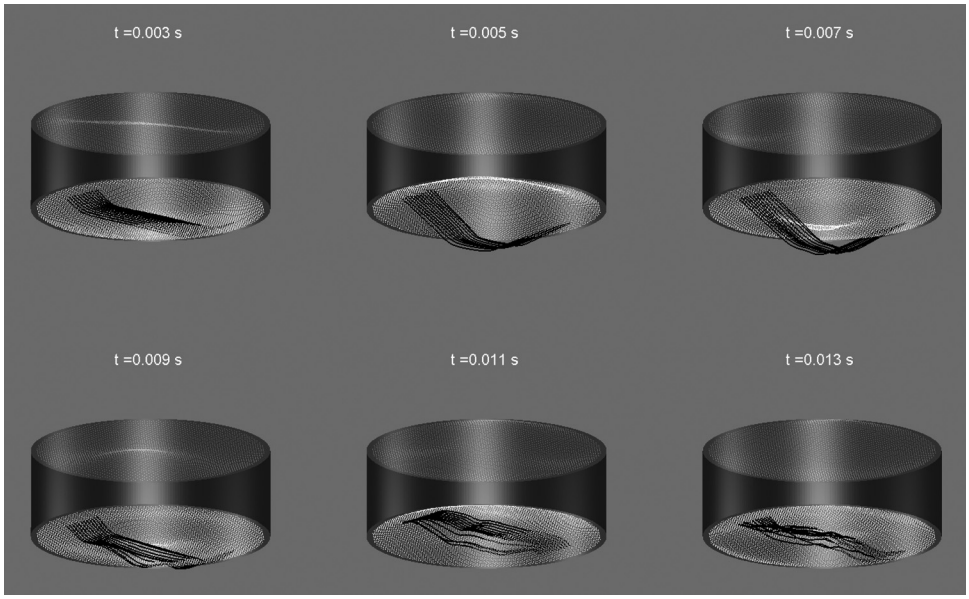


FIG. 10. Snapshots of the response of a coupled membrane system (with snares en gaged) to an short impulsive excitation, viewed from below, at times as indicated.

investigations into coupled mode vibration and acoustic radiation of such structures.

On the other hand, there are many features of snare drums, and drums in general, which have not been adequately modeled here, or removed from consideration for the sake of brevity. The system for the acoustic space should be augmented by terms modeling viscous loss (as, for example, in the model provided in Morse[27]), which has an audible effect

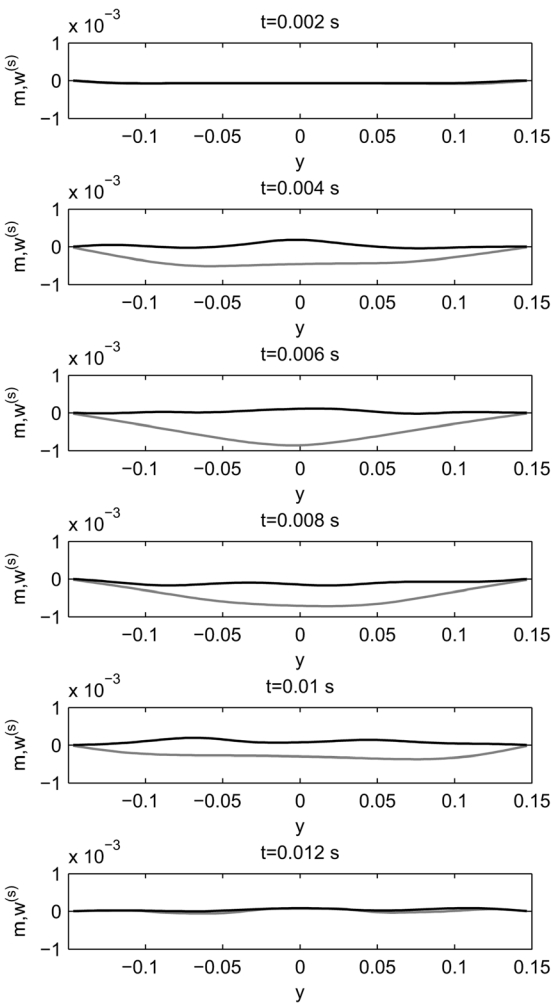


FIG. 11. Snapshots of the interaction between a single snare (in grey) and the snare head, in profile (in black), at times as indicated.

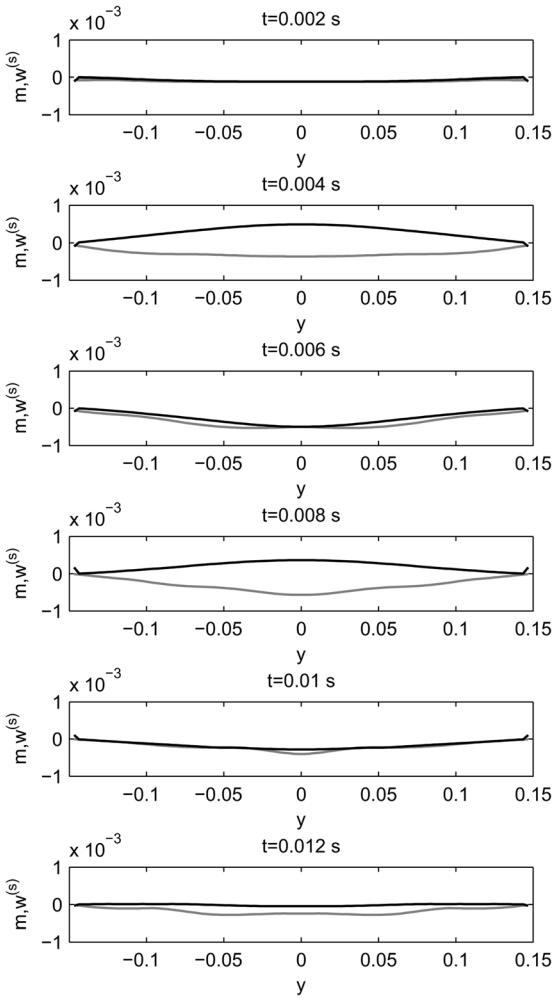


FIG. 12. Snapshots of the interaction between a single snare (in grey) and the snare head, in profile (in black), at times as indicated, for a simplified piston model of the drum cavity.

at high frequencies. Additional terms modeling stiffness, internal losses, and simple nonlinearities have been indicated in Sec. II C, and should be included (in the case of loss, the parameters $\sigma_0$ and $\sigma_1$ must be set via comparison with measurement) in any fine-grained implementation used for experimental comparison. Also missing here is a full model of the shell surrounding the cavity (which may be important as a means of storing energy, if not a significant source of acoustic radiation[1]), as well as a support structure. The excitation signal used here is designed for synthesis applications, and is a simple alternative to a full model of the stick/membrane interaction, as described in Sec. II E. It is useful for single strikes, but certain typical gestures, such as the drum roll, requiring a continuous forcing, are curious examples of an auto-oscillatory system[28] in the world of percussion instruments.

A more general technique highlighted here, in the case of the snare drum (and used previously[10] for the kettledrum) is that of embedding an object in a 3D computational space, so eliminating the need for a general consideration of radiation conditions (in general, simple approximations are only available in cases such as a single membrane in an infinite plane baffle). If the computational region is not too large, then computational expense is not extreme by today's standards. The technique could reasonably be applied for simulation of any acoustic musical instrument.

## ACKNOWLEDGMENTS

Special thanks for the many interesting insights provided by Federico Avanzini, from the University of Padova, during his visit to Edinburgh in November, 2009. The author is also grateful to Antoine Chaigne, for a discussion regarding the excitation mechanism.

[1]T. Rossing, I. Bork, H. Zhao, and D. Fystrom, "Acoustics of snare drums," J. Acoust. Soc. Am. **92**, 84–94 (1992).
[2]T. Rossing, "Acoustics of percussion instruments: Recent progress," Acoust. Sci. & Tech. **22**, 177–188 (2001).
[3]L. Tronchin, "Modal analysis and intensity of acoustic radiation of the kettledrum," J. Acoust. Soc. Am. **117**, 926–933 (2005).
[4]K. Legge and N. Fletcher, "Nonlinearity, chaos, and the sound of shallow gongs," J. Acoust. Soc. Am**. 86**, 2439–2443 (1989).
[5]C. Touzé, O. Thomas, and A. Chaigne, "Asymmetric nonlinear forced vibrations of free-edge circular plates. Part I. Theory," J. Sound Vib. **258**, 649–676 (2002).
[6]J. O. Smith III, *Physical Audio Signal Processing* (DSPRelated.com, Stanford, CA, 2004).
[7]J. Laird, "The physical modeling of drums using digital waveguides," Ph.D. dissertation, University of York (2001).
[8]S. van Duyne and J. O. Smith III, "A simplified approach to modelling dispersion caused by stiffness in strings and plates," in *Proc. Int. Comp. Music Conf.*, Århus, Denmark, (September 12–17, 1994), pp. 407–410.
[9]F. Avanzini and R. Marogna, "A modular physically based approach to the sound syn thesis of membrane percussion instruments," IEEE Trans. Audio, Speech, Lang. Process. **18**, 891–902 (2010).
[10]L. Rhaouti, A. Chaigne, and P. Joly, "Time-domain modeling and numerical simulation of a kettledrum," J. Acoust. Soc. Am. **105**, 3545–3562 (1999).
[11]See supplementary material at E-JASMAN-130-018291 for examples of sound synthesis using the algorithm described, for snare drum synthesis.
[12]P. Morse and U. Ingard, *Theoretical Acoustics* (Princeton University Press, Princeton, New Jersey, 1968), p. 247.
[13]J.-P. Berenger, "Three-dimensional perfectly matched layer for the absorption of electro magnetic waves," J. Comp. Phys. **127**, 363–379 (1996).
[14]F. Hu, "On absorbing boundary conditions for linearized Euler equations by a perfectly matched layer," J. Comp. Phys. **129**, 201–219 (1996).
[15]B. Engquist and A. Majda, "Absorbing boundary conditions for the numerical evaluation of waves," Math. Comput. **31**, 629–651 (1977).
[16]H. Berger, "A new approach to the analysis of large deflections of plates," J. Appl. Math. **22**, 465–472 (1955).
[17]S. Bilbao, *Numerical Sound Synthesis: Finite Difference Schemes and Simulation in Musical Acoustics* (Wiley, Chichester, UK, 2009), p. 361.
[18]C. Erkut, "Aspects in analysis and model-based sound synthesis of plucked string in struments," Ph.D. dissertation, Helsinki University of Technology (2002).
[19]T. Rossing, *The Science of Percussion Instruments* (World Scientific Publishing Company, Singapore, 2000), p. 26.
[20]L. Della Pietra and S. della Valle, "On the dynamic behaviour of axially excited helical springs," Meccanica **17**, 31–43.
[21]A. Chaigne and A. Askenfelt, "Numerical simulations of struck strings. I. A physical model for a struck string using finite difference methods," J. Acoust. Soc. Am. **95**, 1112–1118 (1994).
[22]K. van den Doel and D. Pai, "Modal synthesis for vibrating objects," in *Audio Anecdotes III*, edited by K. Greenebaum (A. K. Peters, Natick, Massachusetts, 2007).
[23]S. Bilbao, *Numerical Sound Synthesis: Finite Difference Schemes and Simulation in Musical Acoustics* (Wiley, Chichester, UK, 2009), p. 354.
[24]J. Strikwerda, *Finite Difference Schemes and Partial Differential Equations* (Wadsworth and Brooks/Cole Advanced Books and Software, Pacific Grove, CA, 1989), p. 47.
[25]S. Bilbao, *Numerical Sound Synthesis: Finite Difference Schemes and Simulation in Musical Acoustics* (Wiley, Chichester, UK, 2009), p. 101.
[26]M. Sosnick and W. Hsu, "Efficient finite difference based synthesis using GPUs," in *Proc. Sound Music Comp. Conf.*, Barcelona, Spain (July 21–24, 2010), paper 71.
[27]P. Morse and U. Ingard, *Theoretical Acoustics* (Princeton University Press, Princeton, NJ, 1968), p. 270.
[28]G. Weinreich, "Mechanical oscillations," in *Mechanics of Musical Instruments*, edited by A. Hirschberg, J. Kergomard, and G. Weinreich, (Springer, New York, 1995), pp. 79–114.